Inorganic Chemistry

Article

pubs.acs.org/IC

Influence of Terminal Acryloyl Arms on the Coordination Chemistry of a Ditopic Pyrimidine–Hydrazone Ligand: Comparison of Pb(II), Zn(II), Cu(II), and Ag(I) Complexes

Daniel J. Hutchinson, Lyall R. Hanton,* and Stephen C. Moratti

Department of Chemistry, University of Otago, P.O. Box 56, Dunedin, New Zealand

Supporting Information

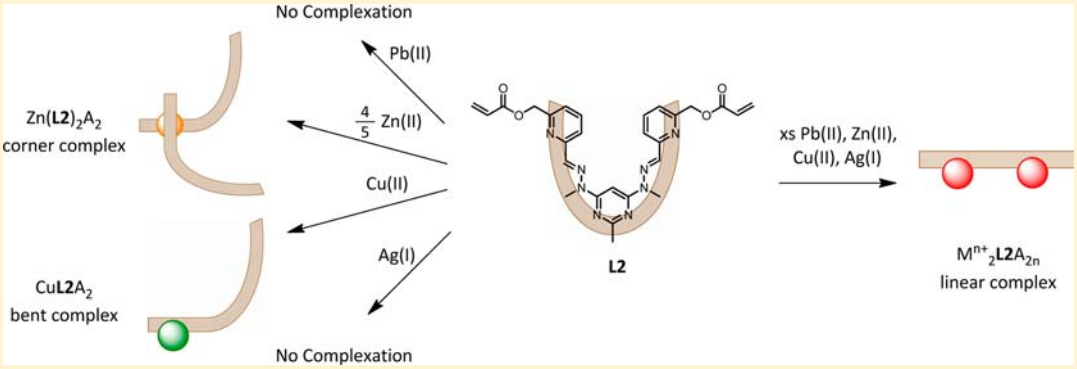

ABSTRACT: A new ditopic pyrimidine–hydrazone ligand, 6-hydroxymethylacryloyl-2-pyridinecarboxaldehyde, 2,2′-[2,2′-(2-methyl-4,6-pyrimidinediyl)bis(1-methylhydrazone)] (**L2**), was synthesized with terminal acryloyl functional groups to allow incorporation into copolymer gel actuators. NMR spectroscopy was used to show that **L2** adopted a horseshoe shape with transoid–transoid pym–hyz–py linkages. Metal complexation studies were performed with **L2** and salts of Pb(II), Zn(II), Cu(II), and Ag(I) ions in CH_3CN in a variety of metal to ligand ratios. Reacting **L2** with an excess amount of any of the metal ions resulted in linear complexes where the pym–hyz–py linkages were rotated to a cisoid–cisoid conformation. NMR spectroscopy showed that the acryloyl arms of **L2** did not interact with the bound metal ions in solution. Seven of the linear complexes (**1**–**7**) were crystallized and analyzed by X-ray diffraction. Most of these complexes (**4**–**7**) also showed no coordination between the acryloyl arms and the metal ions; however, complexes **1**–**3** showed some interactions. Both of the acryloyl arms were coordinated to Pb(II) ions in $[Pb_2\mathbf{L2}(SO_3CF_3)_4]$ (**1**), one through the carbonyl oxygen donor and the other through the alkoxy oxygen donor. One of the acryloyl arms of $[Cu_2\mathbf{L2}(CH_3CN)_3](SO_3CF_3)_4$ (**2**) was coordinated to one of the Cu(II) ions through the carbonyl oxygen donor. There appeared to be a weak association between the alkoxy donors of the acryloyl arms and the Pb(II) ions of $[Pb_2\mathbf{L2}(ClO_4)_4]\cdot CH_3CN$ (**3**). Reaction of excess $AgSO_3CF_3$ with **L2** was repeated in CD_3NO_2, resulting in crystals of $\{[Ag_7(\mathbf{L2})_2(SO_3CF_3)_6(H_2O)_2]\ SO_3CF_3\}_\infty$ (**8**), the polymeric structure of which resulted from coordination between the carbonyl donors of the acryloyl arms and the Ag(I) ions. In all cases the coordination and steric effects of the acryloyl arms did not inhibit isomerization of the pym–hyz bonds of **L2** or the core shape of the linear complexes.

INTRODUCTION

Molecular strands of repeating pyrimidine–hydrazone (pym–hyz) units have been shown to unfold from a helical to a linear shape upon coordination of suitable metal ions.[1] This dynamic structural change arises from rotation of the pym–hyz linkages from their favored transoid conformation to the higher energy cisoid conformation in order to present a tridentate binding site of nitrogen donors to the incoming metal ion.[2] Reversible uncoiling of a variety of pym–hyz helical strands has been induced with metal ions such as Pb(II),[1,3] Zn(II),[1,4−7] Cu(II),[7−9] and Ag(I)[10] ions. The extension of length of the pym–hyz strand upon uncoiling is a motion akin to a one-dimensional molecular motor.[1]

Our research is concerned with harnessing the reversible motion of these pym–hyz strands to power a polymer gel actuator in which the pym–hyz strands would cross-link the polymeric strands of the gel. Such gels have emerged as soft actuating technologies[11] in the realms of robotics[12] and microfluidics[13] due to their ability to absorb solvent and swell in size upon application of an external stimulus.[14] Actuation of the proposed pym–hyz gel would be controlled by the metal-ion-induced conformational change of the pym–hyz cross-linking units within (Figure 1).

In order to incorporate the pym–hyz strands into a polymer gel it is necessary to append suitable functional groups to the terminal pyridine (py) rings used to cap the strands. The acryloyl functional group is a suitable choice since its vinyl

Received: December 20, 2012
Published: February 20, 2013

   dx.doi.org/10.1021/ic3027978 | Inorg. Chem. 2013, 52, 2716–2728

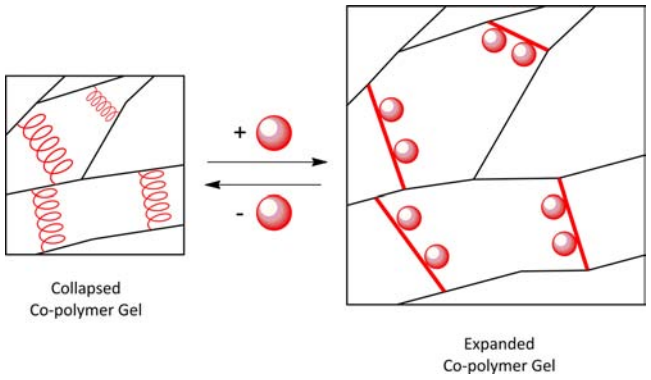

Figure 1. Flow of metal ions in to and out of the copolymer gel results in reversible uncoiling/coiling of the pym−hyz cross-linking units (shown in red), which alters the gels ability to absorb solvent molecules and swell in size.

bond is able to undergo both radical and anionic polymerization.[15] However, it is vital that the added functional groups do not impede the transoid to cisoid conformational change of the pym−hyz strands upon addition of metal ions. Previous work with the ditopic pym−hyz strand **L1**, which contains terminal hydroxymethyl arms, shows that coordination of the appended hydroxymethyl groups through their oxygen donors to Pb(II), Zn(II), Cu(II), and Ag(I) ions does not prevent formation of linear complexes when an excess of metal ions is used.[16−18] However, the interactions of these added functional groups with the metal ions does influence the outcome of self-assembly when a 1:1 metal to ligand ratio is employed (Figure 2).

For example, reacting **L1** with Cu(II) ions in a 1:1 metal to ligand ratio results in bent complexes containing only one Cu(II) ion[18] as opposed to the [2 × 2] square grid complexes which are usually the outcome upon reacting Cu(II) ions with ditopic pym−hyz ligands.[8] A [2 × 2] grid is formed by reacting **L1** with Pb(II) ions in a 1:1 metal to ligand ratio; however, it is severely distorted due to the hydroxymethyl arms crowding the coordination sphere of the Pb(II) ions.[1,17] Although Zn(II) is commonly used to synthesize [2 × 2] grids from ditopic pym−hyz ligands,[5] no such complexes form with **L1** due to coordination of the hydroxymethyl arms. Reacting **L1** with Ag(I) ions in a 1:1 metal to ligand ratio forms double-helicate complexes in solution, which crystallize into either double helicates or side by side dimeric structures depending on the coordinating nature of the solvent (Figure 2).[16]

The acryloyl functional group contains a carbonyl and an alkoxy oxygen donor, both of which could possibly bind to the metal ions attached to the pym−hyz−py coordination pocket. The large steric bulk of the acryloyl arms could also impede access to the pym−hyz−py coordination pocket. These two effects could favor formation of incomplete grids[19] and side by side[20] complexes at metal to ligand ratios of 1:1 as opposed to the [2 × 2] square grids, and double helicates usually formed

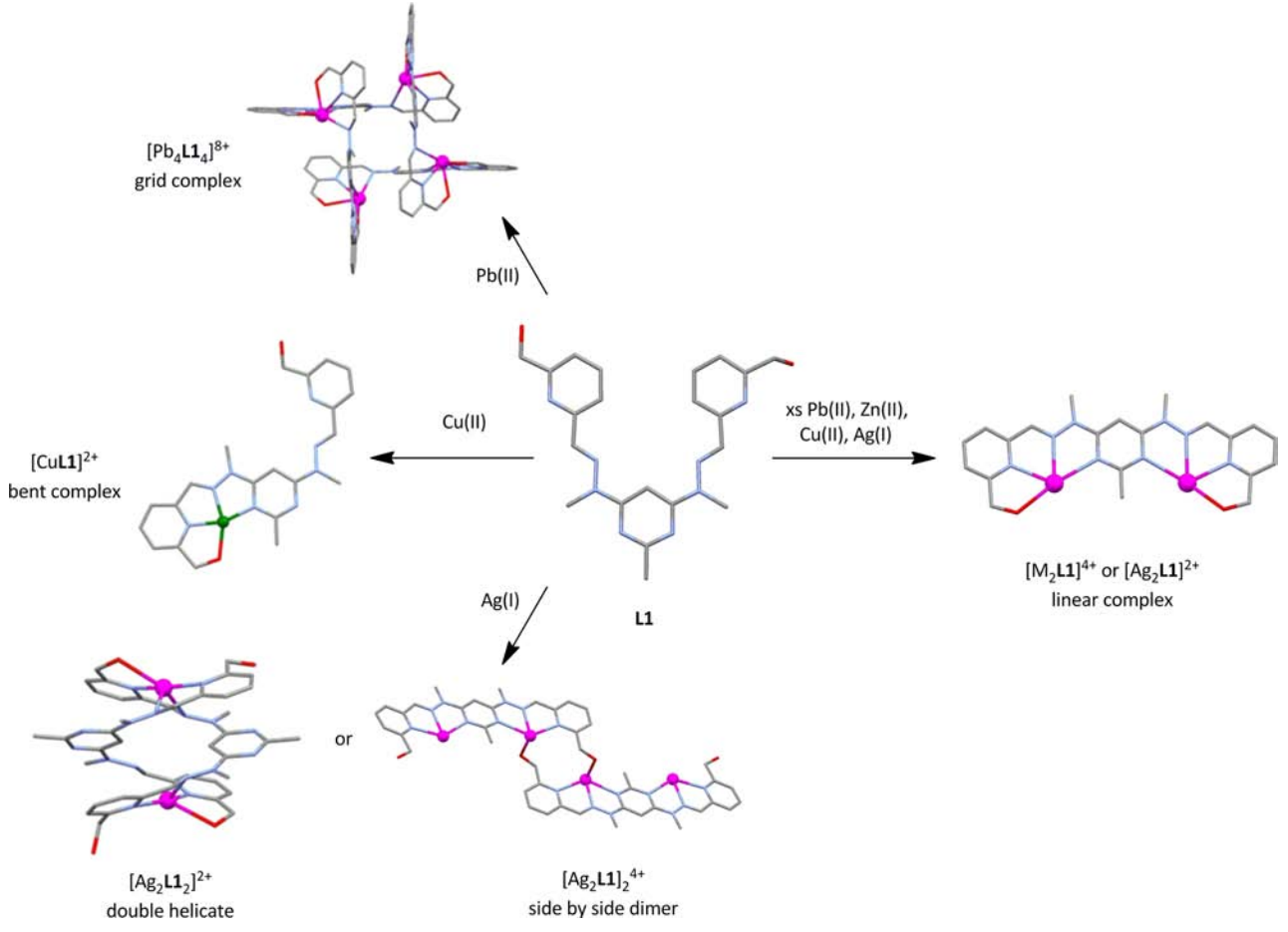

Figure 2. Examples of the shapes of solid state structures synthesized by reacting the ditopic hydroxymethyl terminated pym−hyz ligand **L1** with Pb(II), Zn(II), Cu(II), and Ag(I) ions.[16−18]

dx.doi.org/10.1021/ic3027978 | *Inorg. Chem.* 2013, 52, 2716−2728

Scheme 1. Synthesis of L2 from Reaction of A and B in a 1:2 Molar Ratio in EtOH[a]

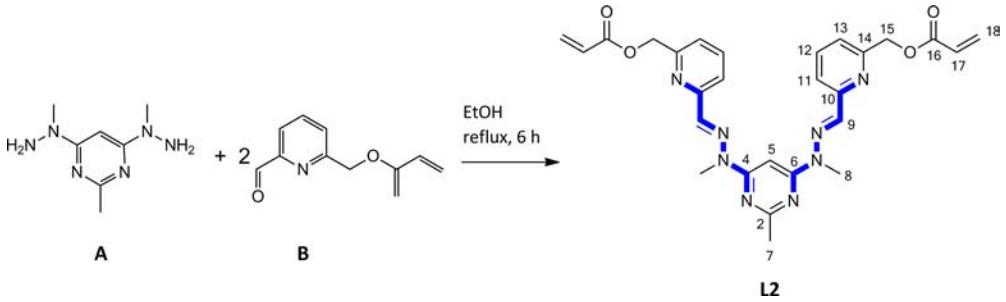

[a]The transoid−transoid pym−hyz−py bonds of **L2** are highlighted (NMR numbering).

with ditopic pym−pyz ligands. It is therefore necessary to characterize the impact that the presence of these terminal groups has on the coordination chemistry of pym−hyz strands. To this end, a ditopic pym−hyz strand containing terminal acryloyl functional groups (**L2**, Scheme 1) has been synthesized and reacted with metal salts of Pb(II), Zn(II), Cu(II), and Ag(I) ions in a variety of metal to ligand ratios. **L2** is a unique ligand in the area of metallosupramolecular chemistry, as demonstrated by the lack of complexes containing terminal acryloyl arms available in the Cambridge Structural Database (CSD version 5.33).[21]

Addition of these metal ions in excess to **L2** resulted in linear complexes in which both pym−hyz bonds were rotated to the cisoid arrangement. NMR spectroscopy showed that the acryloyl arms were not coordinated to the metal ions through either of the oxygen donors in solution and that the coordination environments of the ions were instead completed by solvent molecules. Eight of these linear complexes were crystallized and analyzed by X-ray diffraction, the structures of which showed occasional binding of the acryloyl arms. This coordination, however, merely competed with solvent and anion molecules and did not interfere with the transoid to cisoid isomerization of **L2** or the core complex shape.

Reacting **L2** with either Pb(II) or Ag(I) ions in a 1:1 metal to ligand ratio only resulted in linear complexes and unreacted ligand material. Mono-Cu(II) complexes were formed, and it was assumed that they had a bent shape similar to those formed with **L1**.[18] Although no complexes were formed with **L1** and Zn(II) ions in a 1:1 metal to ligand ratio, **L2** and Zn(II) ions formed corner complexes in a 4:5 metal to ligand ratio which were fully characterized by NMR spectroscopy.

EXPERIMENTAL SECTION

General. All starting materials, reagents, and metal salts were purchased from commercial sources and used as received without further purification, with the exception of $Pb(SO_3CF_3)_2{\cdot}H_2O$ and $Cu(SO_3CF_3)_2{\cdot}4H_2O$, which were produced through treatment of $2PbCO_3{\cdot}Pb(OH)_2$ and $CuCO_3{\cdot}Cu(OH)_2{\cdot}H_2O$, respectively, with aqueous triflic acid. Precursors 4,6-bis(1-methylhydrazino)-2-methylpyrimidine (**A**)[22] and 2-propenoic acid, (6-formyl-2-pyridinyl)methyl ester (**B**),[23] were prepared according to their literature methods. All solvents were used as received and of LR grade or better.

Microanalyses were carried out in the Campbell Microanalytical Laboratory, University of Otago. All measured microanalysis results had an uncertainty of ±0.4%. ^{1}H and ^{13}C NMR spectra and two-dimensional (gCOSY, NOSEY, HSQC, gHMBC) spectra were collected on a 500 MHz Varian UNITY INOVA spectrometer at 298 K. Spectra were collected in $CDCl_3$, CD_3CN, or CD_3NO_2 and referenced to the internal solvent signal, with chemical shifts reported in δ units (ppm). Electrospray mass spectrometry (ESMS) was carried out on a Bruker microTOFQ instrument (Bruker Daltronics, Bremen, Germany). Samples were introduced using direct infusion into an ESI source in positive mode. Sampling was averaged for 2 min over a m/z range of 50−3000 amu. Mass was calibrated using an external calibrant of sodium formate clusters, 15 calibration points from 90 to 1050 amu, using a quadratic plus HPC line fit. ESMS spectra were processed using Compass software (version 1.3, Bruker Daltronics, Bremen, Germany). Infrared (IR) spectra were recorded on a Bruker Alpha-P ATR-IR spectrometer. UV−vis spectra were recorded on an Agilent 8453 spectrophotometer against a CH_3CN background using quartz cells with a 1 cm path length.

Synthesis of 6-Hydroxymethylacryloyl-2-pyridinecarboxaldehyde, 2,2′-[2,2′-(2-Methyl-4,6-pyrimidinediyl)bis(1-methylhydrazone)] (L2). A solution of **A** (0.805 g, 4.42 mmol) and **B** (1.71 g, 8.94 mmol) in EtOH (100 mL) was refluxed for 6 h. Over the course of the reaction a white solid precipitated out of solution. The mixture was filtered, and the solid was washed with EtOH and dried in vacuo for 2 days to give **L2** as a white solid (1.85 g, 79%). Mp 177−179 °C. Anal. Calcd for $C_{27}H_{28}N_8O_4$: C, 61.30; H, 5.34; N, 21.20. Found: C, 61.22; H, 5.39; N, 21.45. ^{1}H NMR (500 MHz, $CDCl_3$) δ/ppm: 8.08 (2H, d, J = 7.9 Hz, H11), 7.83 (2H, s, H9), 7.73 (3H, t, J = 7.8 Hz, H5/H12), 7.30 (2H, d, J = 7.5 Hz, H13), 6.53 (2H, dd, J = 1.4, 17.3 Hz, H18a), 6.26 (2H, dd, J = 10.4, 17.3 Hz, H17), 5.92 (2H, dd, J = 1.4, 10.4 Hz, H18b), 5.35 (4H, s, H15), 3.69 (6H, s, H8), 2.55 (3H s, H7). ^{13}C NMR (500 MHz, $CDCl_3$) δ/ppm: 163.8 (C2), 163.5 (C16), 160.6 (C6), 153.1 (C14), 152.7 (C10), 134.4 (C12), 133.9 (C9), 129.3 (C18), 125.7 (C17), 118.6 (C13), 116.3 (C11), 83.8 (C5), 64.4 (C15), 27.4 (C8), 23.8 (C7). ESMS m/z found: 529.2303, 551.2139, 567.1871. Calcd for $C_{27}H_{29}N_8O_4^+$: 529.58. Selected IR ν/cm^{-1}: 3421 (m, br), 2922 (m, CH str), 1721 (s, C═O str), 1636 (m, C═C str), 1593 (s), 1563 (s, C═N str), 1487 (s), 1458 (s), 1411 (s), 1397 (s), 1301 (s), 1269 (s, CO str), 1170 (m), 1091 (m), 1050 (m).

Pb_2L2$(SO_3CF_3)_4$. $Pb(SO_3CF_3)_2{\cdot}H_2O$ (91.5 mg, 0.175 mmol) in CH_3CN (5.00 mL) was added to **L2** (45.9 mg, 0.0869 mmol), resulting in complete dissolution of the ligand material with stirring at 75 °C. The clear, yellow reaction solution was then stirred with diethyl ether (20.0 mL), resulting in precipitation of a yellow solid. This solid was isolated by filtration, washed with diethyl ether, and dried in vacuo (64.3 mg, 48%). Anal. Calcd for $C_{31}H_{28}N_8O_{16}F_{12}S_4Pb_2$: C, 24.19; H, 1.83; N, 7.28. Found: C, 24.24; H, 1.99; N, 7.30. ^{1}H NMR (400 MHz, CD_3CN) δ/ppm: 8.90 (2H, s, H9), 8.29 (2H, t, J = 7.8 Hz, H12), 8.05 (2H, d, J = 7.7 Hz, H11), 7.89 (2H, d, J = 7.8 Hz, H13), 6.77 (1H, s, H5), 6.52 (2H, dd, J = 1.0, 17.3 Hz, H18a), 6.36 (2H, dd, J = 10.4, 17.3 Hz, H17), 6.02 (2H, dd, J = 1.1, 10.4 Hz, H18b), 5.55 (4H, s, H15), 3.79 (6H, s, H8), 2.94 (3H, s, H7). ESMS m/z Found: 529.2432. Calcd for $C_{27}H_{29}N_8O_4^+$: 529.2311. Selected IR ν/cm^{-1}: 3400 (w), 1714 (m, C═O str), 1617 (w, C═C str), 1589 (m), 1550 (s, C═N str), 1490 (m), 1459 (m), 1408 (m), 1391 (m), 1291 (s), 1229 (s), 1206 (s), 1156 (s), 1047 (s), 1013 (s). Crystals suitable for X-ray diffraction were grown by slow diffusion of diethyl ether into a CH_3CN solution of $Pb(SO_3CF_3)_2$ and **L2** in a 2:1 metal to ligand ratio. These crystals gave the structure $[Pb_2L2(SO_3CF_3)_4]$ (**1**).

Cu_2L2$(SO_3CF_3)_4$. $Cu(SO_3CF_3)_2{\cdot}4H_2O$ (65.1 mg, 0.150 mmol) in CH_3CN (5.00 mL) was added to a suspension of **L2** (39.3 mg, 0.0744

dx.doi.org/10.1021/ic3027978 | Inorg. Chem. 2013, 52, 2716−2728

mmol) in CH_3CN (5.00 mL) with stirring at 75 °C. This resulted in complete dissolution of the ligand material and formation of a clear, green solution. This solution was stirred in diethyl ether (20.0 mL), resulting in precipitation of a green solid, which was isolated by filtration, washed with diethyl ether, and dried in vacuo (51.9 mg, 56%): Anal. Calcd for $C_{31}H_{28}N_8O_{16}F_{12}S_4Cu_2{\cdot}H_2O$: C, 29.32; H, 2.38; N, 8.82. Found: C, 29.26; H, 2.50; N, 8.85. Selected IR ν/cm^{-1}: 3055 (w, C−H str), 1726 (m, C═O str), 1658 (m, C═C str), 1633 (m), 1589 (s), 1560 (s, C═N str), 1497 (m), 1470 (m), 1434 (m), 1414 (m), 1388 (w), 1238 (s), 1223 (s, $SO_3CF_3^-$), 1156 (s), 1063 (s), 1025 (s). UV−vis $\lambda_{max}(\varepsilon)$/nm(L mol^{-1} cm^{-1}): 696 (297). Single crystals suitable for X-ray diffraction were grown through slow diffusion of diethyl ether into a CH_3CN solution of $Cu(ClO_4)_2{\cdot}6H_2O$ and **L2**. These crystals gave the structure $[Cu_2\mathbf{L2}(CH_3CN)_3](SO_3CF_3)_4$ (**2**).

Pb_2L2$(ClO_4)_4$. $Pb(ClO_4)_2{\cdot}3H_2O$ (105 mg, 0.229 mmol) in CH_3CN (5.00 mL) was added to **L2** (56.5 mg, 0.107 mmol), resulting in complete dissolution of the ligand material with stirring at 75 °C. The clear, yellow reaction solution was then stirred with diethyl ether (20.0 mL), resulting in precipitation of a yellow solid. This solid was isolated by filtration, washed with diethyl ether, and dried in vacuo (44.0 mg, 31%). Anal. Calcd for $C_{27}H_{28}N_8O_{20}Cl_4Pb_2{\cdot}2H_2O$: C, 23.55; H, 2.34; N, 8.14. Found: C, 23.60; H, 2.39; N, 8.00. ^{1}H NMR (500 MHz, CD_3CN) δ/ppm: 8.95 (2H, s, H9), 8.30 (2H, t, J = 7.8 Hz, H12), 8.09 (2H, d, J = 7.6 Hz, H11), 7.90 (2H, d, J = 7.7 Hz, H13), 6.80 (1H, s, H5), 6.52 (2H, dd, J = 1.1, 17.3 Hz, H18a), 6.36 (2H, dd, J = 10.4, 17.3 Hz, H17), 6.03 (2H, dd, J = 1.1, 10.4 Hz, H18b), 5.54 (4H, s, H15), 3.82 (6H, s, H8), 2.94 (3H, s, H7). ^{13}C NMR (500 MHz, CD_3CN) δ/ppm: 168.09 (C2), 166.89 (C16), 160.99 (C4/6), 157.71 (C14), 150.31 (C10), 147.38 (C9), 143.26 (C12), 134.28 (C18), 130.13 (C11), 128.79 (C13), 128.66 (C17), 87.92 (C5), 66.61 (C15), 36.57 (C8), 26.67 (C7). ESMS m/z Found: 529.2452. Calcd for $C_{27}H_{29}N_8O_4^+$: 529.2311. Selected IR ν/cm^{-1}: 3417 (w), 1715 (m, C═O str), 1617 (w, C═C str), 1591 (s), 1551 (s, C═N str), 1494 (m), 1459 (m), 1435 (m), 1408 (m), 1391 (m), 1301 (m), 1268 (m), 1161 (s), 1039 (s, br). Yellow crystals suitable for X-ray diffraction were grown by slow diffusion of diethyl ether into a CH_3CN solution of $Pb(ClO_4)_2{\cdot}3H_2O$ and **L2** in a 2:1 metal to ligand ratio. These crystals gave the structure $[Pb_2\mathbf{L2}(ClO_4)_4]{\cdot}CH_3CN$ (**3**).

Zn_2L2$(SO_3CF_3)_4$. $Zn(SO_3CF_3)_2$ (70.1 mg, 0.193 mmol) in CH_3CN (5.00 mL) was added to a suspension of **L2** (49.1 mg, 0.0930 mmol) in CH_3CN (5.00 mL) with stirring at 75 °C. This resulted in complete dissolution of the ligand material and formation of a clear, yellow solution. The solution was reduced in volume by rotary evaporation and then stirred in diethyl ether (20.0 mL), resulting in precipitation of a yellow solid. This solid was isolated by filtration, washed with diethyl ether, and dried in vacuo (73.0 mg, 64%). Anal. Calcd for $C_{31}H_{28}N_8O_{16}F_{12}S_4Zn_2{\cdot}2H_2O$: C, 28.83; H, 2.50; N, 8.68. Found: C, 29.10; H, 2.87; N, 8.79. ^{1}H NMR (500 MHz, CD_3CN) δ/ppm: 8.43 (2H, s, H9), 8.29 (2H, t, J = 7.8 Hz, H12), 7.94 (2H, d, J = 7.6 Hz, H11), 7.91 (2H, d, J = 7.9 Hz, H13), 6.81 (1H, s, H5), 6.57 (2H, dd, J = 1.0, 17.3 Hz, H18a), 6.36 (2H, dd, J = 10.5, 17.3 Hz, H17), 6.08 (2H, dd, J = 1.0, 10.5 Hz, H18b), 5.60 (4H, s, H15), 3.81 (6H, s, H8), 3.09 (3H, s, H7). ^{13}C NMR (500 MHz, CD_3CN) δ/ppm: 168.88 (C2), 167.50 (C16), 159.36 (C4/6), 158.35 (C14), 147.45 (C10), 143.59 (C12), 138.83 (C9), 133.97 (C18), 128.26 (C17), 128.13 (C11), 127.51 (C13), 86.70 (C5), 66.00 (C15), 34.70 (C8), 26.75 (C7). ESMS m/z Found: 637.1426, 529.2246. Calcd for $C_{27}H_{29}N_8O_4^+$: 529.2312. Selected IR ν/cm^{-1}: 3239 (w), 1733 (w, C═O str), 1664 (w), 1632 (w, C═C str), 1587 (s), 1559 (s, C═N str), 1491 (m), 1466 (m), 1436 (m), 1415 (m), 1392 (m), 1288 (s), 1262 (s), 1204 (s), 1156 (s), 1059 (s), 1021 (s). Yellow crystals suitable for X-ray diffraction were grown by slow diffusion of diethyl ether into a CH_3CN solution of $Zn(SO_3CF_3)_2$ and **L2** in a 2:1 metal to ligand ratio. These crystals gave the structure $[Zn_2\mathbf{L2}(SO_3CF_3)_3(CH_3CN)_2(H_2O)]SO_3CF_3{\cdot}H_2O$ (**4**).

Zn_2L2$(BF_4)_4$. $Zn(BF_4)_2$ (203 mg, 0.851 mmol) in CH_3CN (4.00 mL) was added to a suspension of **L2** (109 mg, 0.206 mmol) in CH_3CN (4.00 mL) with stirring at 75 °C. This resulted in complete dissolution of the ligand material and formation of a clear, yellow solution. The solution was reduced in volume by rotary evaporation and then stirred in diethyl ether (20.0 mL), resulting in precipitation of a yellow solid. This solid was isolated by filtration, washed with diethyl ether, and dried in vacuo (0.1660 g, 80%). Anal. Calcd for $C_{27}H_{28}N_{16}O_4B_4F_{16}Zn_2{\cdot}H_2O$: C, 31.70; H, 2.96; N, 10.96. Found: C, 31.95; H, 3.15; N, 10.79. ^{1}H NMR (400 MHz, CD_3CN) δ/ppm: 8.39 (2H, s, H9), 8.26 (2H, t, J = 7.8 Hz, H12), 7.91 (2H, d, J = 7.6 Hz, H11), 8.87 (2H, d, J = 7.9 Hz, H13), 6.75 (1H, s, H5), 6.55 (2H, dd, J = 1.1, 17.3 Hz, H18a), 6.35 (2H, dd, J = 10.4, 17.3 Hz, H17), 6.06 (2H, dd, J = 1.1, 10.4 Hz, H18b), 5.56 (4H, s, H15), 3.79 (6H, s, H8), 2.97 (3H, s, H7). ESMS m/z Found: 529.2374. Calcd for $C_{27}H_{29}N_8O_4$: 529.2311. Selected IR ν/cm^{-1}: 3458 (w, br), 1727 (w, C═O str), 1663 (w), 1633 (w, C═C str), 1588 (s), 1560 (s, C═N str), 1491 (m), 1466 (m), 1437 (m), 1411 (m), 1393 (m), 1293 (m), 1262 (m), 1161 (m), 977 (s, br). Yellow crystals suitable for X-ray diffraction were grown by slow diffusion of diethyl ether into a CH_3CN solution of $Zn(BF_4)_2$ and **L2** in a 4:1 metal to ligand ratio. These crystals gave the structure $[Zn_2\mathbf{L2}(BF_4)_3(H_2O)]$-$BF_4{\cdot}CH_3CN{\cdot}H_2O$ (**5**).

Cu_2L2$(ClO_4)_4$. $Cu(ClO_4)_2{\cdot}6H_2O$ (59.9 mg, 0.161 mmol) in CH_3CN (5.00 mL) was added to a suspension of **L2** (41.8 mg, 0.0792 mmol) in CH_3CN (5.00 mL) with stirring at 75 °C. This resulted in complete dissolution of the ligand material and formation of a clear, green solution. This solution was stirred in diethyl ether (20.0 mL), resulting in precipitation of a green solid, which was isolated by filtration, washed with diethyl ether, and dried in vacuo (50.2 mg, 60%). Anal. Calcd for $C_{27}H_{28}N_8O_{20}Cl_4Cu_2{\cdot}3CH_3CN{\cdot}H_2O$: C, 33.18; H, 3.29; N, 12.90. Found: C, 33.02; H, 3.56; N, 12.41. Selected IR ν/cm^{-1}: 3055 (w, C−H str), 2934 (w, C−H str), 2313 (w), 2285 (w), 1727 (m, C═O str), 1632 (m, C═C str), 1605 (m), 1587 (s), 1561 (s, C═N str), 1489 (m), 1402 (m), 1390 (m), 1292 (m, C−O str), 1262 (m), 1188 (m), 1057 (s, br, ClO_4^-), 1014 (s). UV−vis $\lambda_{max}(\varepsilon)$/nm ($L$ mol^{-1} cm^{-1}): 689 (320). Single crystals suitable for X-ray diffraction were grown through slow diffusion of diethyl ether into a CH_3CN solution of $Cu(ClO_4)_2{\cdot}6H_2O$ and **L2**. These crystals gave the structure $[Cu_2\mathbf{L2}(ClO_4)(CH_3CN)_3](ClO_4)_3$ (**6**).

Ag_2L2$(SO_3CF_3)_2$. $AgSO_3CF$ (87.3 mg, 0.341 mmol) in CH_3CN (2.00 mL) was added to **L2** (43.9 mg, 0.0831 mmol), resulting in complete dissolution of the ligand material with stirring at 75 °C and formation of a clear, yellow solution. This solution was stirred in diethyl ether (20.0 mL), causing precipitation of a yellow solid, which was then washed with diethyl ether and dried in vacuo (42.7 mg, 49%). Anal. Calcd for $C_{29}H_{28}N_8O_{10}F_6S_2Ag_2{\cdot}H_2O$: C, 32.85; H, 2.85; N, 10.57. Found: C, 32.87; H, 2.73; N, 10.75. ^{1}H NMR (500 MHz, CD_3CN) δ/ppm: 7.96 (2H, s, H9), 7.94 (2H, t, J = 7.8 Hz, H12), 7.59 (2H, d, J = 7.8 Hz, H11), 7.55 (2H, d, J = 7.7 Hz, H13), 6.49 (2H, dd, J = 1.6, 15.6 Hz, H18a), 6.47 (1H, s, H5), 6.29 (2H, dd, J = 10.4, 17.3 Hz, H17), 5.99 (2H, dd, J = 1.2, 10.5 Hz, H18b), 5.45 (4H, s, H15), 3.57 (6H, s, H8), 2.82 (3H, s, H7). ^{13}C NMR (500 MHz, CD_3CN) δ/ppm: 168.43 (C2), 166.77 (C16), 161.30 (C4/6), 158.04 (C14), 150.54 (C10), 140.86 (C12), 137.19 (C9), 132.99 (C18), 129.03 (C17), 127.15 (C13), 124.47 (C11), 87.32 (C5), 67.76 (C15), 34.39 (C8), 29.17 (C7). ESMS m/z Found: 1163.3491, 635.1316. Calcd for $(C_{27}H_{28}N_8O_4)_2Ag^+$: 1163.3518. Calcd for $C_{27}H_{28}N_8O_4Ag^+$: 635.1284. Selected IR ν/cm^{-1}: 3468 (w), 3061 (w, C−H str), 2952 (w, C−H str), 1720 (m, C═O str), 1579 (m), 1546 (s, C═N str), 1483 (m), 1457 (m), 1430 (m), 1405 (m), 1350 (m), 1282 (s, C−O str), 1233 (s), 1220 (s, $SO_3CF_3^-$), 1179 (s), 1153 (s), 1066 (s), 1046 (s), 1023 (s). Yellow crystals suitable for X-ray determination were grown by slow diffusion of diethyl ether into a CH_3CN solution of $AgSO_3CF_3$ and **L2** in a 4:1 metal to ligand ratio. These crystals gave the structure $[Ag_2\mathbf{L2}(SO_3CF_3)(CH_3CN)_3]SO_3CF_3$ (**7**).

The reaction was repeated in CD_3NO_2 (0.75 mL) with $AgSO_3CF_3$ (24.9 mg, 0.0969 mmol) and **L2** (12.9 mg, 0.0244 mmol), resulting in complete dissolution of the ligand material with stirring at 95 °C and formation of a clear yellow solution. ^{1}H NMR (400 MHz, CD_3NO_2) δ/ppm: 8.23(2H, s, H9), 8.13 (2H, t, J = 7.8 Hz, H12), 7.73 (2H, d, J = 7.8 Hz, H11), 7.68 (2H, d, J = 7.9 Hz, H13), 6.85 (1H, s, H5), 6.51 (2H, d, J = 17.3 Hz, H18a), 6.28 (2H, dd, J = 10.4, 17.3 Hz, H17), 6.02 (2H, d, J = 10.4 Hz, H18b), 5.30 (4H, s, H15), 3.79 (6H, s, H8),

dx.doi.org/10.1021/ic3027978 | Inorg. Chem. 2013, 52, 2716−2728

Table 1. Crystallographic Data for Complexes of L2

	[Pb_2**L2**$(SO_3CF_3)_4$] (**1**)	[Cu_2**L2**$(CH_3CN)_3$]$(SO_3CF_3)_4$ (**2**)	[Pb_2**L2**$(ClO_4)_4$]· CH_3CN (**3**)
formula	$C_{31}H_{28}F_{12}N_8O_{16}Pb_2S_4$	$C_{33}H_{37}Cu_2N_{11}O_4$	$C_{29}H_{31}Cl_4N_9O_{20}Pb_2$
fw	1539.23	778.84	1381.83
cryst syst	triclinic	triclinic	triclinic
space group	*P*-1	*P*-1	*P*-1
a/Å	10.9614(5)	13.2961(9)	13.3813(5)
b/Å	14.1662(6)	13.8546(9)	13.6338(5)
c/Å	16.4345(7)	16.5011(12)	14.6157(6)
α/deg	102.640(3)	86.432(3)	117.6600(10)
β/deg	104.898(3)	82.154(3)	92.1710(10)
γ/deg	100.224(3)	73.922(3)	115.2450(10)
V/Å^3	2331.31(19)	2892.5(3)	2041.48(14)
Z	2	2	2
T/K	90(2)	90(2)	90(2)
μ/mm^{-1}	7.515	0.768	8.591
no. of reflns collected	27 213	26 515	26 459
no. of unique reflns (R_{int})	8638 (0.0381)	9192 (0.0520)	6916 (0.0292)
R_1 indices [$I > 2\sigma(I)$]	0.0557	0.0763	0.0202
w*R*2 (all data)	0.1575	0.2318	0.0432
goodness of fit	1.064	1.089	1.032

	[Zn_2**L2**$(SO_3CF_3)_3(CH_3CN)_2$ (H_2O)]SO_3CF_3·H_2O (**4**)	[Zn_2**L2**$(BF_4)_3(H_2O)$]BF_4· CH_3CN·H_2O (**5**)	[Cu_2**L2**$(ClO_4)(CH_3CN)_3$] $(ClO_4)_3$ (**6**)
formula	$C_{35}H_{36}F_{12}N_{10}O_{18}S_4Zn_2$	$C_{29}H_{33}B_4F_{16}N_9O_6Zn_2$	$C_{33}H_{35}Cl_4Cu_2N_{11}O_{20}$
fw	1371.72	1081.62	1174.60
cryst syst	triclinic	monoclinic	triclinic
space group	*P*-1	$P2_1$	*P*-1
a/Å	11.7789(6)	10.4633(11)	12.742(4)
b/Å	14.4891(7)	15.6954(16)	14.056(4)
c/Å	17.0456(9)	13.1984(12)	15.538(4)
α/deg	92.881(3)	90	111.517(10)
β/deg	108.955(3)	106.125(4)	103.767(11)
γ/deg	98.791(3)	90	104.831(11)
V/Å^3	2703.5(4)	2082.2(6)	2326.1(12)
Z	2	2	2
T/K	90(2)	90(2)	90(2)
μ/mm^{-1}	1.159	1.277	1.233
no. of reflns collected	19 039	33 121	32 463
no. of unique reflns (R_{int})	9934 (0.0482)	5511 (0.0553)	8188 (0.0361)
R_1 indices [$I > 2\sigma(I)$]	0.1055	0.0388	0.0549
w*R*2 (all data)	0.2511	0.0901	0.1540
goodness of fit	1.116	1.091	1.116

	[Ag_2**L2**$(SO_3CF_3)(CH_3CN)_3$] SO_3CF_3 (**7**)	{[Ag_7(**L2**$)_2(SO_3CF_3)_6(H_2O)_2$] SO_3CF_3}$_\infty$ (**8**)
formula	$C_{35}H_{37}Ag_2F_6N_{11}O_{10}S_2$	$C_{30}H_{28}Ag_{3.50}F_9N_8O_{14}S_3$
fw	1165.64	1369.33
cryst syst	triclinic	triclinic
space group	*P*-1	*P*-1
a/Å	11.9718(4)	11.7250(9)
b/Å	12.9367(5)	13.5150(11)
c/Å	15.4355(6)	16.5799(13)
α/deg	84.843(2)	104.351(4)
β/deg	68.834(2)	94.273(4)
γ/deg	79.247(2)	96.468(4)
V/Å^3	2189.50(14)	2514.8(5)
Z	2	2
T/K	90(2)	90(2)
μ/mm^{-1}	1.083	1.566
no. of reflns collected	33 806	24 608
no. of unique reflns (R_{int})	12 714 (0.0411)	7908 (0.0381)
R_1 indices [$I > 2\sigma(I)$]	0.0362	0.0550
w*R*2 (all data)	0.1057	0.1649
goodness of fit	1.113	1.062

dx.doi.org/10.1021/ic3027978 | *Inorg. Chem.* 2013, 52, 2716−2728

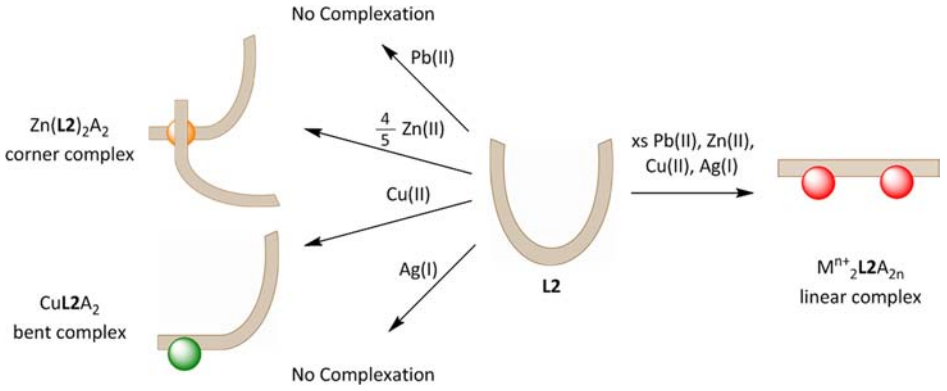

Figure 3. Schematic summarizing complexes of **L2** formed through reactions with Pb(II), Zn(II), Ag(I), and Cu(II) salts in CH_3CN in a variety of different metal to ligand ratios (A = ClO_4^-, $SO_3CF_3^-$, or BF_4^-; n = metal-ion charge).

2.80 (3H, s, H7). Yellow crystals suitable for X-ray determination were grown by slow evaporation of this CD_3NO_2 solution. These crystals gave the structure $\{[Ag_7(\mathbf{L2})_2(SO_3CF_3)_6(H_2O)_2]SO_3CF_3\}_\infty$ (**8**).

$Zn(L2)_2(SO_3CF_3)_2$. $Zn(SO_3CF_3)_2$ (33.8 mg, 0.132 mmol) in CD_3CN (0.75 mL) was added to **L2** (85.1 mg, 0.161 mmol), resulting in complete dissolution with agitation at 75 °C. The clear, yellow reaction solution was then stirred in diethyl ether (20.0 mL), resulting in precipitation of a yellow solid. This solid was isolated by filtration, washed with diethyl ether, and dried in vacuo (27.9 mg, 24%). Anal. Calc. for $C_{56}H_{56}N_{16}O_{14}F_6S_2Zn\cdot{}^1/_3Zn(SO_3CF_3)_2$: C, 44.14; H, 3.66; N, 14.54. Found: C, 44.54; H, 3.74; N, 14.68. ^{1}H NMR (500 MHz, CD_3CN) δ/ppm: 8.66 (1H, s, H9A), 8.17 (1H, d, J = 7.6 Hz, H13B), 8.13 (1H, t, J = 7.8 Hz, H12A), 7.99 (1H, s, H9B), 7.92 (2H, m, H11A/H12B), 7.70 (1H, d, J = 7.8 Hz, H13A), 7.44 (1H, d, J = 7.7 Hz, H11B), 7.32 (1H, s, H5), 6.44 (1H, dd, J = 1.4, 17.3 Hz, H18Aa), 6.35 (1H, dd, J = 1.2, 17.3 Hz, H18Bb), 6.25 (1H, dd, J = 10.4, 17.3 Hz, H17A), 6.08 (1H, dd, J = 10.5, 17.3 Hz, H17B), 5.95 (1H, dd, J = 1.4, 10.4 Hz, H18Ab), 5.90 (1H, dd, J = 1.2, 10.5 Hz, H18Bb), 5.28 (2H, s, H15B), 4.79 (2H, d, J = 2.3 Hz, H15A), 4.03 (3H, s, H8A), 3.64 (3H, s, H8B), 2.11 (3H, s, H7). ^{13}C NMR (500 MHz, CD_3CN) δ/ppm: 167.97 (C2), 166.91 (C16A), 166.50 (C16B), 164.71 (C6), 159.11 (C14A), 158.63 (C4), 157.40 (C14B), 154.57 (C10B), 148.12 (C10A), 143.41 (C9B), 142.88 (C12A), 140.16 (C9A), 139.13 (C12B), 133.63 (C18B), 132.71 (C18A), 129.31 (C11A), 128.56 (C17B), 127.44 (C13A), 123.42 (C11B), 121.14 (C13B), 87.04 (C5), 67.73 (C15B), 65.22 (C15A), 35.65 (C8A), 30.90 (C8B), 26.06 (C7). ESMS m/z Found: 551.2036, 529.2190. Calcd for $C_{27}H_{28}N_8O_4Na^+$: 551.2131. Calcd for $C_{27}H_{29}N_8O_4^+$: 529.2312. Selected IR ν/cm^{-1}: 3492 (w, br), 3042 (w, C−H str), 2930 (w, C−H str), 1720 (m, C═O str), 1587 (s), 1548 (s, C═N str), 1487 (m), 1455 (m), 1404 (m), 1252 (s), 1222 (s), 1157 (s), 1121 (s), 1090 (s), 1049 (s), 1026 (s).

$Zn(L2)_2(BF_4)_2$. $Zn(BF_4)_2$ (28.0 mg, 0.117 mmol) in CH_3CN (4.00 mL) was added to a suspension of **L2** (81.0 mg, 0.153 mmol) in CH_3CN (4.00 mL) with stirring at 75 °C. This resulted in complete dissolution of the ligand material and formation of a clear, yellow solution. The solution was reduced in volume by rotary evaporation and then stirred in diethyl ether (20.0 mL), resulting in precipitation of a yellow solid. This solid was isolated by filtration, washed with diethyl ether, and dried in vacuo (39.4 mg, 44%). Anal. Calcd for $C_{54}H_{56}N_{16}O_4B_2F_8Zn\cdot{}^1/_4Zn(BF_4)_2$: C, 47.84; H, 4.16; N, 16.53. Found: C, 47.73; H, 4.24; N, 16.50. ^{1}H NMR (400 MHz, CD_3CN) δ/ppm: 8.58 (1H, s, H9A), 8.17 (1H, d, J = 7.9 Hz, H13B), 8.13 (1H, t, J = 7.8 Hz, H12A), 8.01 (1H, s, H9B), 7.92 (1H, t, J = 7.8 Hz, H12B), 7.88 (1H, d, J = 7.7 Hz, H11A), 7.69 (1H, d, J = 7.9 Hz, H13A), 7.46 (1H, d, J = 7.7 Hz, H11B), 7.31 (1H, s, H5), 6.45 (1H, dd, J = 1.4, 17.3 Hz, H18Aa), 6.35 (1H, J = 1.2, 17.4 Hz, H18Ba), 6.26 (1H, dd, J = 10.4, 17.4 Hz, H17A), 6.08 (2H, dd, J = 10.5, 17.3 Hz, H17B), 5.96 (1H, dd, J = 1.4, 10.4 Hz, H18Ab), 5.90 (1H, dd, J = 1.2, 10.5 Hz, H18Bb), 5.30 (2H, s, H15B), 4.77 (2H, d, J = 2.2 Hz, H15A), 4.00 (3H, s, H8A), 3.66 (3H, s, H8B), 2.09 (3H, s, H7). ESMS m/z Found: 627.1242, 551.2135, 529.2364. Calcd for $C_{27}H_{28}N_8O_4ZnCl^+$: 627.1213. Calcd for $C_{27}H_{28}N_8O_4Na^+$: 551.2131. Calcd for $C_{27}H_{29}N_8O_4^+$: 529.2312. Selected IR ν/cm^{-1}: 3067 (w, C−H str), 2922 (w, C−H str), 1720 (m, C═O str), 1588 (m), 1550 (s, C═N str), 1486 (m), 1450 (m), 1405 (m), 1296 (m), 1264 (m), 1232 (m), 1168 (m), 1123 (m), 1047 (s).

$CuL2(ClO_4)_2$. $Cu(ClO_4)_2\cdot 6H_2O$ (33.7 mg, 0.0911 mmol) in CH_3CN (5.00 mL) was added to a suspension of **L2** (47.6 mg, 0.0901 mmol) in CH_3CN (5.00 mL) stirring at 75 °C. This resulted in complete dissolution of the ligand material and formation of a clear, green solution. This solution was stirred in diethyl ether (20.0 mL), resulting in precipitation of a green solid, which was isolated by filtration, washed with diethyl ether, and dried in vacuo (45.6 mg, 64%). Anal. Calcd for $C_{27}H_{28}N_8O_{12}Cl_2Cu$: C, 41.00; H, 3.57; N, 14.17. Found: C, 40.80; H, 3.81; N, 13.91. Selected IR: 3067 (w, C−H str), 2944 (w, C−H str), 1721 (m, C═O str), 1583 (s), 1553 (s, C═N str), 1492 (m), 1456 (m), 1405 (m), 1295 (m, C−O str), 1257 (m), 1161 (s), 1077 (s), 1049 (s, br, ClO_4^-). UV−vis $\lambda_{max}(\varepsilon)$/nm(L mol^{-1} cm^{-1}): 652 (198).

$CuL2(SO_3CF_3)_2$. $Cu(SO_3CF_3)_2\cdot 4H_2O$ (30.8 mg, 0.0711 mmol) in CH_3CN (5.00 mL) was added to a suspension of **L2** (37.1 mg, 0.0703 mmol) in CH_3CN (5.00 mL) stirring at 75 °C. This resulted in complete dissolution of the ligand material and formation of a clear, green solution. This solution was stirred in diethyl ether (20.0 mL), resulting in precipitation of a green solid, which was isolated by filtration, washed with diethyl ether, and dried in vacuo (14.1 mg, 23%). Anal. Calcd for $C_{29}H_{28}N_8O_{10}F_6S_2Cu\cdot 2H_2O$: C, 37.60; H, 3.48; N, 12.10. Found: C, 37.60; H, 3.47; N, 11.85. Selected IR ν/cm^{-1}: 3055 (w, C−H str), 29.0 (w, C−H str), 1719 (m, C═O str), 1662 (w, C═C str), 1589 (s), 1546 (s, C═N str), 1493 (m), 1457 (m), 1413 (m), 1280 (s, C−O str), 1233 (s, $SO_3CF_3^-$), 1157 (s), 1119 (s), 1057 (s), 1024 (s). UV−vis λ_{max} (ε)/nm (L mol^{-1} cm^{-1}): 656 (223).

X-ray Crystallography. Crystallographic data are summarized in Table 1. Thermal ellipsoid pictures of complexes **1**−**8** and selected bond lengths and angles are available in the Supporting Information along with a description of how the disordered components of the complexes were treated. X-ray diffraction data were collected on a Bruker APEX II CCD diffractometer, with graphite-monochromated Mo Kα (λ = 0.71073 Å) radiation. Intensities were corrected for Lorentz polarization effects,[24] and a multiscan absorption correction[25] was applied. Structures were solved by direct methods (SHELXS[26] or SIR-97[27]) and refined on F^2 using all data by full-matrix least-squares procedures (SHELXL 97[28]). All calculations were performed using the WinGX interface.[29] Detailed analyses of the extended structure were carried out using PLATON[30] and MERCURY[31] (Version 2.4).

RESULTS AND DISCUSSION

Synthesis and Structure of L2. The ditopic pym−hyz ligand **L2** was designed with acryloyl arms attached to the terminal py rings in order to allow incorporation of the ligand into a copolymer gel through radical polymerization.[15] **L2** was

dx.doi.org/10.1021/ic3027978 | Inorg. Chem. 2013, 52, 2716−2728

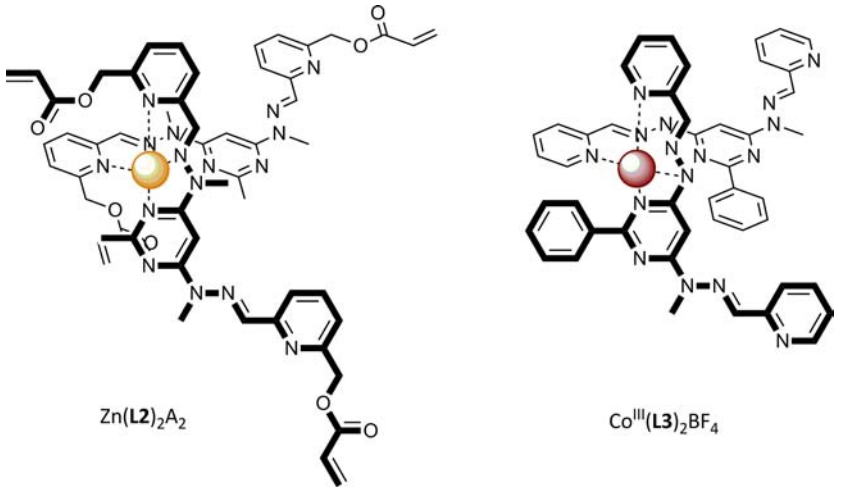

Figure 4. Comparison of the corner complexes formed with Zn(II) ions and **L2**, with the $[Co^{III}(\mathbf{L3})_2]BF_4$ corner complex from the literature, made with an asymmetric ditopic pym−hyz ligand **L3**.[7]

synthesized through a double imine condensation reaction between 4,6-bis(1-methylhydrazino)pyrimidine (**A**) and 2-propenoic acid, (6-formyl-2-pyridinyl)methyl ester (**B**), in a 1:2 molar ratio (Scheme 1). The reaction was performed in EtOH under refluxing conditions and resulted in precipitation of **L2** from the reactant solution as a pure white solid during the reaction.

The ESMS spectrum of **L2** showed peaks due to molecular ions $[\mathbf{L2} + H]^+$ and $[\mathbf{L2} + Na]^+$, while the IR spectrum of the ligand showed a strong peak at 1721 cm^{-1} due to the C═O stretching mode of the terminal acryloyl arms and a C═N stretching mode at 1560 cm^{-1}. A sample of **L2** was dissolved in $CDCl_3$ for analysis by ^1H and ^{13}C NMR spectroscopy, which confirmed the horseshoe-like shape of the ligand and the transoid−transoid conformation of the pym−hyz−py linkages. This was evident from the NOE correlations between H5 and H11 and the lack of correlation between H5 and H8 and H9 and H11 (Scheme 1). The conformation of the pym−hyz bonds was also elucidated from the high chemical shift of the H5 signal, located at 7.73 ppm, as these bonds are known to have a deshielding affect on this proton signal in their transoid conformation only.[1,32] The proton signals from the terminal acryloyl arms occurred as a series of three double doublets between 5.92 and 6.53 ppm in the ^1H NMR spectrum of **L2**.

Synthesis and Structures of Complexes. **L2** was reacted with CH_3CN solutions of the following metal salts: $Pb(ClO_4)_2{\cdot}3H_2O$, $Pb(SO_3CF_3)_2{\cdot}H_2O$, $Zn(SO_3CF_3)_2$, $Zn(BF_4)_2$, $AgSO_3CF_3$, $Cu(ClO_4)_2{\cdot}6H_2O$, and $Cu(SO_3CF_3)_2{\cdot}4H_2O$, in various metal to ligand ratios (Figure 3). Most of these reactions resulted in complete dissolution of the ligand material with stirring and heat. Addition of diethyl ether to the reaction solutions resulted in precipitation of the complexes. These precipitates were analyzed by microanalysis, ESMS, and IR spectroscopy. Crystals were grown by addition of diethyl ether by vapor diffusion and analyzed by X-ray crystallography. The Pb(II), Zn(II), and Ag(I) reactions were repeated in CD_3CN, so the composition of the solutions could be probed by NMR spectroscopy. The Cu(II) reaction solutions were analyzed by UV−vis spectroscopy.

Employing a metal to ligand ratio of 2:1 resulted in linear complexes of the type $M^{n+}{}_2\mathbf{L2}A_{2n}$ (where A = ClO_4^-, $SO_3CF_3^-$, or BF_4^-; n = metal-ion charge) when using either Pb(II) or Cu(II) salts or $Zn(SO_3CF_3)_2$. A 4:1 metal to ligand ratio was necessary to form this type of complex with either $Zn(BF_4)_2$ or $AgSO_3CF_3$. $AgSO_3CF_3$ was also reacted with **L2** in CD_3NO_2 in a variety of metal to ligand ratios, resulting in formation of the linear $Ag_2\mathbf{L2}(SO_3CF_3)_2$ at a metal to ligand ratio of 4:1 and incomplete dissolution of **L2** at all ratios lower than 4:1.

At metal to ligand ratios of 1:1 or lower the resulting complex architectures were found to be dependent on the metal ion used (Figure 3). Typically, when employing 1:1 metal to ligand ratios, ditopic pym−hyz ligands form [2 × 2] square grids when reacted with Pb(II), Zn(II). or Cu(II) ions[1,4,8] and double helicate complexes when reacted with Ag(I) ions.[10] Reacting **L2** with either Pb(II) or Ag(I) at a 1:1 metal to ligand ratio simply resulted in incomplete dissolution of **L2**, with the only complex present in the solution phase being the $M^{n+}{}_2\mathbf{L2}A_{2n}$ linear complex, as identified by NMR spectroscopy. Complete dissolution of **L2** was achieved with either of the Cu(II) salts in a 1:1 metal to ligand ratio, resulting in green solutions of monocopper complexes of type $Cu\mathbf{L2}A_2$. The exact shape of the $Cu\mathbf{L2}A_2$ complexes could not be confirmed as crystals suitable for X-ray analysis were not obtained; however, they are assumed to have a bent shape in an analogous fashion to the mono-Cu(II) complexes of the ditopic hydroxymethyl-terminated pym−hyz ligand **L1**.[18]

Reacting **L2** with either of the Zn(II) salts resulted in complete dissolution at a metal to ligand ratio of 4:5. NMR spectroscopy showed the orange reaction solutions exclusively contained $Zn(\mathbf{L2})_2A_2$ corner-type complexes in which two bent-shaped **L2** ligands shared a single Zn(II) ion. The shape of these complexes was similar to that described in the literature for complex $[Co^{III}(\mathbf{L3})_2]^+$, which contained an asymmetrical ditopic pym−hyz ligand with one ternary hyz nitrogen deprotonated (Figure 4).[7]

Analysis of Complexes. ESMS spectra of the Pb(II) and Zn(II) complexes only showed a peak due to the $[\mathbf{L2} + H]^+$ molecular ion, while the $Ag_2\mathbf{L2}(SO_3CF_3)_2$ complex showed a peak due to the $[Ag\mathbf{L2}]^+$ molecular ion. Cu(II) complexes displayed differing ESMS spectra, containing peaks due to the $[Cu\mathbf{L2}]^+$, $[Cu\mathbf{L2}Cl]^+$, and $[Cu\mathbf{L2}(ClO_4)]^+$ molecular ions. IR spectra of all complexes were similar with each spectrum showing a C═O stretching mode between 1715 and 1733 cm^{-1} and a C═N stretching mode between 1546 and 1561 cm^{-1}. The similarly of the C═O stretching mode frequency between the complexes and **L2** suggested that the acryloyl arms

dx.doi.org/10.1021/ic3027978 | Inorg. Chem. 2013, 52, 2716−2728

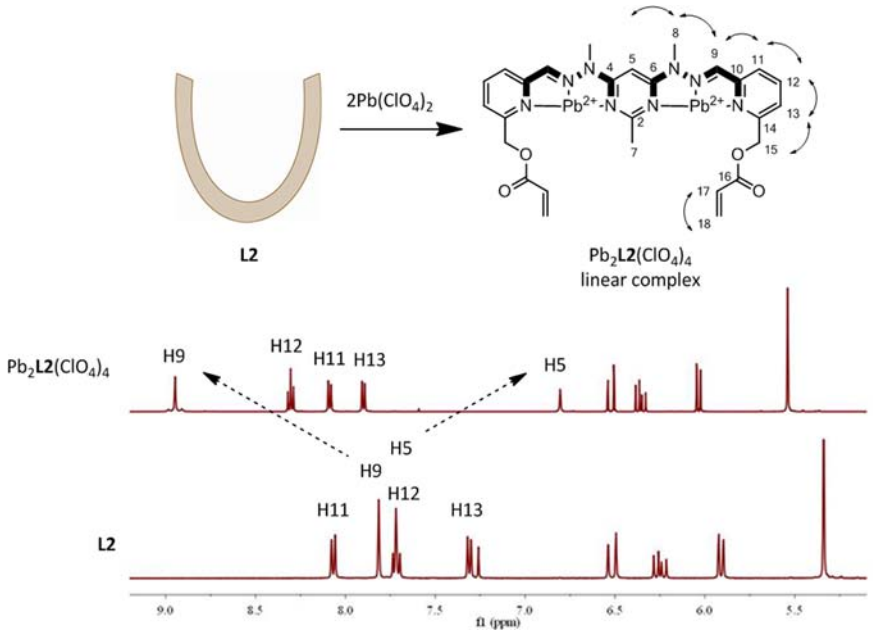

Figure 5. Comparison of the ^{1}H NMR spectra of **L2** and the linear Pb_2**L2**$(ClO_4)_4$ complex, showing the changes in chemical shift of the pym, hyz, and py protons which are witnessed upon forming the linear $M^{n+}{}_2$**L2**A_{2n} complexes. Chemical shifts of the acryloyl protons were unaffected by coordination of Pb(II) ions.

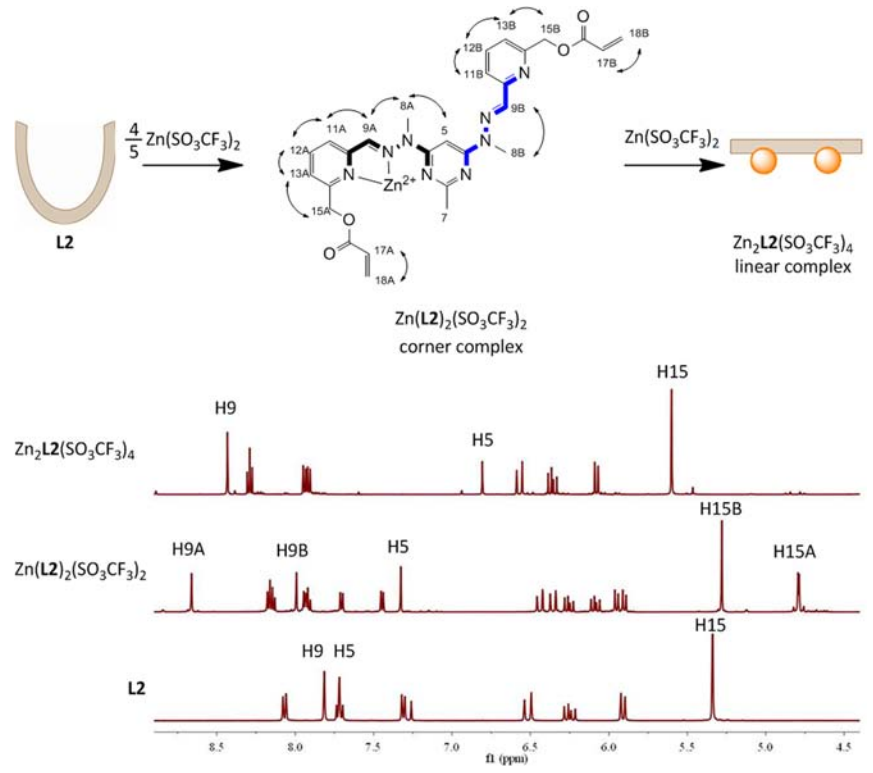

Figure 6. Comparison of the ^{1}H NMR spectra of **L2** and the corner $Zn(\mathbf{L2})_2(SO_3CF_3)_2$ and linear Zn_2**L2**$(SO_3CF_3)_4$ complexes, showing changes in chemical shift of the pym, hyz, and methylene proton signals. NOE correlations for each **L2** molecule in the corner complex are shown.

were not affected by the coordination of the metal ions, while the slight decrease in frequency of the C═N stretching mode from the ligand to the complexes suggested that the binding of metal ions had a small strengthening effect on the imine linkages of **L2**.

The UV−vis spectra of the Cu_2**L2**$(ClO_4)_4$ and Cu_2**L2**$(SO_3CF_3)_4$ complexes each showed a broad featureless d−d transition with λ_{max} values of 689 and 696 nm, respectively, consistent with Cu(II) ions in distorted trigonal bipyramidal or octahedral environments.[33] The d−d transitions of the Cu**L2**$(ClO_4)_2$ and Cu**L2**$(SO_3CF_3)_2$ complexes occurred at 652 and 656 nm, respectively. These wavelengths were consistent with Cu(II) ions in either a distorted octahedral or square pyramidal geometry[33] and were similar to the λ_{max} values

dx.doi.org/10.1021/ic3027978 | Inorg. Chem. 2013, 52, 2716−2728

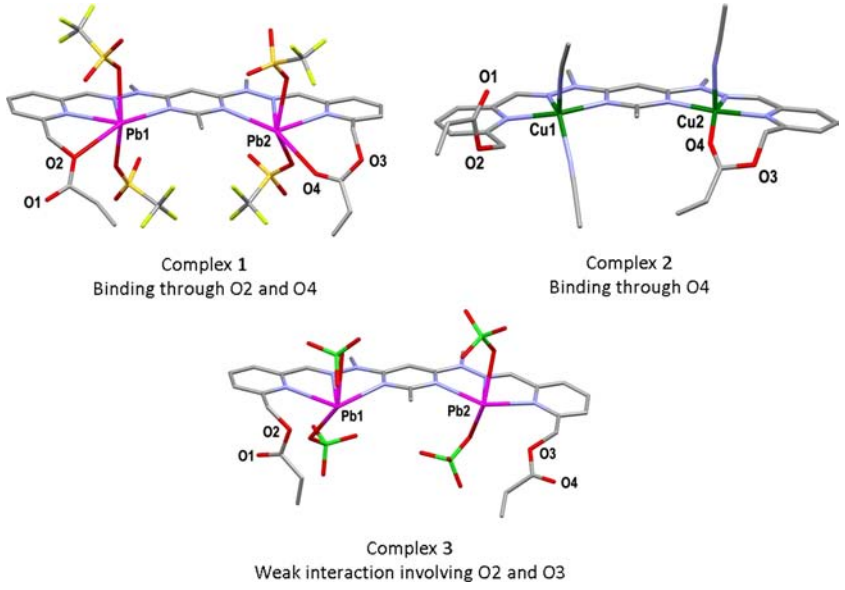

Figure 7. View of the $[Pb_2\mathbf{L2}(SO_3CF_3)_4]$, $[Cu_2\mathbf{L2}(CH_3CN)_3]^{4+}$, and $[Pb_2\mathbf{L2}(ClO_4)_4]$ molecules of complexes **1**, **2**, and **3**, respectively, showing the coordination environments of the metal ions and binding of the acryloyl arms (hydrogens have been omitted for clarity, crystallographic numbering).

of the d−d transitions displayed by the bent mono-Cu(II) complexes of **L1**.[18]

NMR Spectroscopy of Complexes. ^{1}H NMR spectra of the $M^{n+}{}_2\mathbf{L2}A_{2n}$ complexes were all similar to each other, regardless of whether the complexes contained Pb(II), Zn(II), or Ag(I) ions. The choice of counterion also had no bearing on the NMR spectra of the complexes. Each of the linear complexes showed 11 signals, indicating that they were each symmetrical about a mirror plane through the central pym ring. Their linear shape and the cisoid−cisoid pym−hyz−py bond conformations were confirmed by NOE correlations which ran along the backbone of the complexes from H5 through to H15 (Figure 5).

The H5 proton signal was shifted upfield from 7.73 ppm in the ^{1}H NMR spectrum of **L2** to between 6.47 and 6.81 ppm in the spectra of the linear complexes due to removal of the deshielding effects of the pym−hyz bond upon its rotation from transoid to cisoid.[1,32] The binding of metal ions to the nitrogen donors of the pym−hyz−py coordination pockets of **L2** also resulted in the downfield shift of the H9 and pyridine proton signals (Figure 5). The magnitude of these shifts was greatest for the $Pb_2\mathbf{L2}A_4$ complexes and smallest for the $Ag_2\mathbf{L2}(SO_3CF_3)_2$ complex. The chemical shifts of the acryloyl proton signals H17 and H18 were unaffected by the coordination of Pb(II), Zn(II), or Ag(I) ions, suggesting that the acryloyl arms were not coordinated to the metal ions in solution.

NMR spectra of the $Zn(\mathbf{L2})_2(SO_3CF_3)_2$ and $Zn(\mathbf{L2})_2(BF_4)_2$ complexes were identical to each other and showed unambiguously that they consisted of two bent molecules of **L2** sharing a Zn(II) ion (Figure 4). Each of the ^{1}H NMR spectra showed 20 signals, indicating the **L2** molecules in the $Zn\mathbf{L2}_2A_2$ complexes were asymmetric. 2D NOESY spectra showed NOE correlations running along the ligand backbones from H5 to H13A, indicating these halves of the **L2** molecules were linear and had cisoid pym−hyz and hyz−py linkages. The other halves of the **L2** ligands maintained their transoid−transoid conformation as demonstrated by the lack of NOE correlations between H5 and H8B and H9B and H11B (Figure 6). Coordination of the Zn(II) ion to the hyz nitrogen donor on the H5−H13A half of the ligand resulted in deshielding of the H9A protons, while the signal from the H9B protons on the transoid half of the **L2** molecules had a similar chemical shift to that seen in the spectrum of the free ligand. The H5 pym signal had a chemical shift of 7.32 ppm, which was between the chemical shifts of 7.73 and 6.80 ppm in the spectrum of **L2** and its Pb(II) complexes, due to it being between one cisoid and one transoid pym−hyz linkage.

Steric interactions between the two molecules of **L2** in the $Zn(\mathbf{L2})_2A_2$ complexes resulted in the H15A methylene protons experiencing slightly different chemical environments. The H15A signal was therefore a pair of singlets, separated by 2.3 Hz. These signals occurred at a chemical shift of 4.79 ppm, which was much lower than that of the methylene protons of **L2** or any of the linear $M^{n+}{}_2\mathbf{L2}A_{2n}$ complexes. It therefore appeared that the corner shape of the complexes led to shielding of the H15A environment. The other methylene proton signal, H24, was similar to the methylene proton signal in **L2**, as it was a singlet at 5.28 ppm (Figure 6).

X-ray Crystallography. X-ray-quality crystals were grown by slow diffusion of diethyl ether into CH_3CN solutions of the $M^{n+}{}_2\mathbf{L2}A_{2n}$ complexes. These crystals yielded the structures **1**−**7**, all of which were linear in shape with cisoid−cisoid pym−hyz−py bonds and a metal ion bound to the three nitrogen donors of each pym−hyz−py coordination pocket. The main difference between the complexes was the degree of binding between the oxygen donors of the acryloyl arms and the metal ions and the orientation of the terminal acryloyl arms with regard to the rest of the **L2** ligand. The positioning of the arms is described for complexes **1**−**7** in terms of the angle at which the planes of the acryloyl arms bisected the mean plane of the central pym ring of the complex. None of the complexes showed any intermolecular interactions as the acryloyl arms did not participate in H-bonding and their positioning relative to the rest of the complex molecules disrupted any potential $\pi-\pi$ stacking.

Diethyl ether was also slowly diffused into a CD_3NO_2 solution of $AgSO_3CF_3$ and **L2** in a 4:1 metal to ligand ratio.

dx.doi.org/10.1021/ic3027978 | Inorg. Chem. 2013, 52, 2716−2728

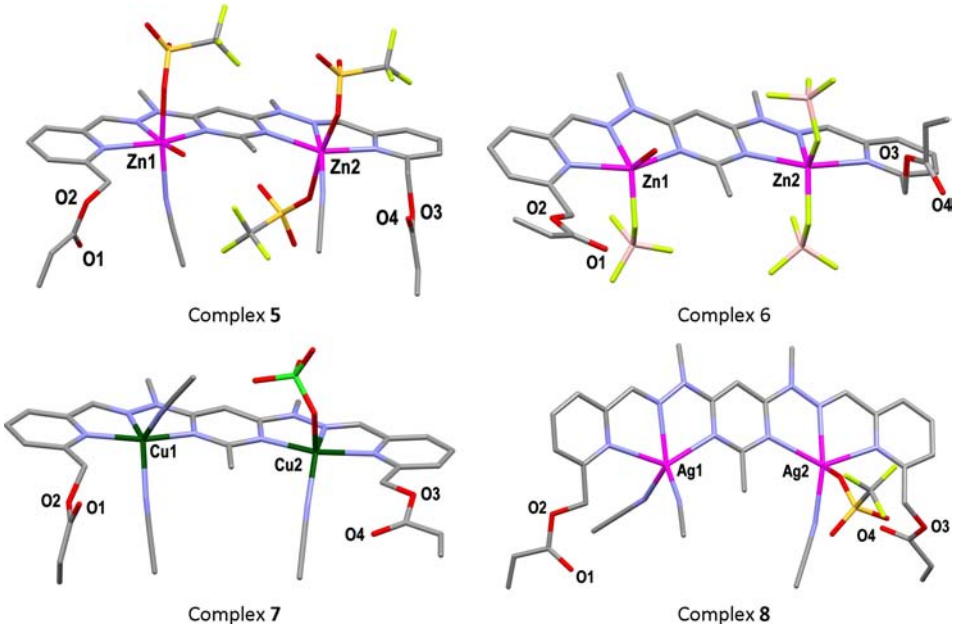

Figure 8. View of the cations of complexes **4**–**7** showing the coordination environments of the metal ions and orientation of the unbound acryloyl arms (hydrogens have been omitted for clarity, crystallographic numbering).

This resulted in formation of the coordination polymer $\{[Ag_7(\mathbf{L2})_2(SO_3CF_3)_6(H_2O)_2]SO_3CF_3\}_\infty$ (**8**). While Ag(I) ions are commonly used in the synthesis of coordination polymers,[34,35] this complex is the first such example of a coordination polymer involving pym–hyz ligands and Ag(I) ions.[10]

Complexes 1–3: Binding of the Acryloyl Arms. Complexes **1**–**3** all showed some interaction between the acryloyl arms and the metal ions occupying the pym–hyz–py coordination pockets (Figure 7). In the $[Pb_2\mathbf{L2}(SO_3CF_3)_4]$ molecule of complex **1**, Pb1 was bound to the carbonyl donor of the nearby acryloyl arm (O1) while Pb2 was bound to the alkoxy oxygen donor (O3). The distances of these coordination bonds were 2.673(10) and 2.832(10) Å, respectively. One of the acryloyl arms in the $[Cu_2\mathbf{L2}(CH_3CN)_3]^{4+}$ cation of complex **2** was bound to Cu2 through the carbonyl donor (O4), while the other acryloyl arm was unbound and protruded out above the mean plane of the complex at an angle of 89.7°. The Cu2–O4 distance was 2.024(5) Å. The acryloyl arms of the $[Pb_2\mathbf{L2}(ClO_4)_4]$ molecule of complex **3** were both positioned such that the alkoxy oxygen donors were orientated toward the Pb(II) ions. However, the Pb1···O2 and Pb2···O3 distances of 2.954(5) and 3.039(5) Å were considered too long for a formal coordination bond and therefore suggested a weak interaction instead [based on a CSD search of Pb···O distances; 6853 bond distances from 1512 complexes with a mean value of 2.59 Å, ranging from 2.01 to 3.45 Å].[21]

The centroid to centroid distances between the terminal py rings of complexes **1** and **3** were 14.03 and 13.99 Å, respectively. The distance across complex **2** was shorter at 12.76 Å due to complex **2** having a slightly curved shape within the mean plane of the pym ring. Each of the Pb(II) ions in complex **1** existed in six-coordinate geometries which resembled distorted pentagonal bipyramidal environments due to the presence of a stereochemically active lone pair of electrons on the Pb(II) ions.[36] Pb(II) ions in complex **3** were five coordinate and had geometries which resembled distorted octahedra due to each ion having a stereochemically active lone pair of electrons. Cu1 and Cu2 ions in complex **2** displayed distorted square pyramidal geometries, with τ_5 values of 0.46 and 0.01, respectively.[37]

Complexes 4–7: No Binding of the Acryloyl Arms. The acryloyl arms in complexes **4**–**7** were consistently positioned such that the carbonyl and alkoxy oxygen donors were orientated away from the metal ions. The majority of the unbound acryloyl arms protruded out of the mean plane of the pym ring at angles ranging from 73.4° to 87.2° in a similar fashion to the unbound arm of complex **2**. The O1-containing acryloyl arms of complexes **5** and **7** and the O3-containing arm of complex **6** extended out from their py rings at gentler angles of 22.0°, 57.7°, and 20.9°, respectively (Figure 8).

Complexes **4** and **5** were slightly bowed out of the mean plane of the central pym ring and as a result were shorter than complexes **1** and **3**, with lengths of 13.38 and 13.45 Å, respectively. The distance across complex **6** was 12.87 Å, which was similar to that of complex **2** due to **6** also having a slightly curved shape within the mean plane. The distance across complex **7** was equivalent to the lengths of complexes **1** and **3** at 13.95 Å.

Due to the lack of metal-ion binding of the acryloyl arms in complexes **4**–**7** the coordination spheres of the metal ions were completed with solvent and/or counterions. The Zn(II) ions in complex **4** adopted distorted six-coordinate octahedral geometries, while in complex **5** the five-coordinate Zn1 and Zn2 ions existed in distorted trigonal bipyramidal (τ_5 = 0.57) and distorted square pyramidal (τ_5 = 0.42)[37] environments, respectively. In complex **6** the five-coordinate Cu1 and Cu2 ions also adopted a distorted trigonal bipyramidal geometry (τ_5 = 0.54) and a distorted square pyramidal environment (τ_5 = 0.40),[37] respectively. Ag(I) ions of complex **7** both displayed square pyramidal geometries with τ_5 values of 0.04 and 0.32, respectively.[37]

Complex 8: $\{[Ag_7(L2)_2(SO_3CF_3)_6(H_2O)_2]SO_3CF_3\}_\infty$. Crystals of complex **8** were grown through slow evaporation of a CD_3NO_2 solution of **L2** and $AgSO_3CF_3$ in a 4:1 metal to ligand ratio. The asymmetric unit consisted of a **L2** molecule and 3.5

dx.doi.org/10.1021/ic3027978 | *Inorg. Chem.* 2013, 52, 2716–2728

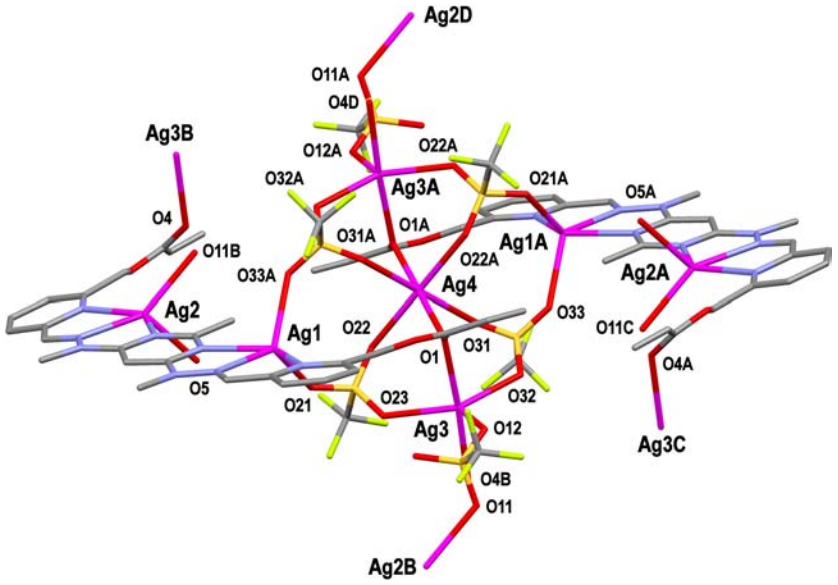

Figure 9. View of the $[Ag_7(\mathbf{L2})_2(SO_3CF_3)_6(H_2O)_2]^+$ cation of complex **8**, including the Ag2−O11 and Ag3−O4 coordination bonds which linked the dimers of **8** into a one-dimensional chain (hydrogens have been omitted for clarity; symmetry code A $2-x, 2-y, z$; B $x, -1+y, z$; C $2-x, 1-y, -z$; D $2-x, 3-y, -z$).

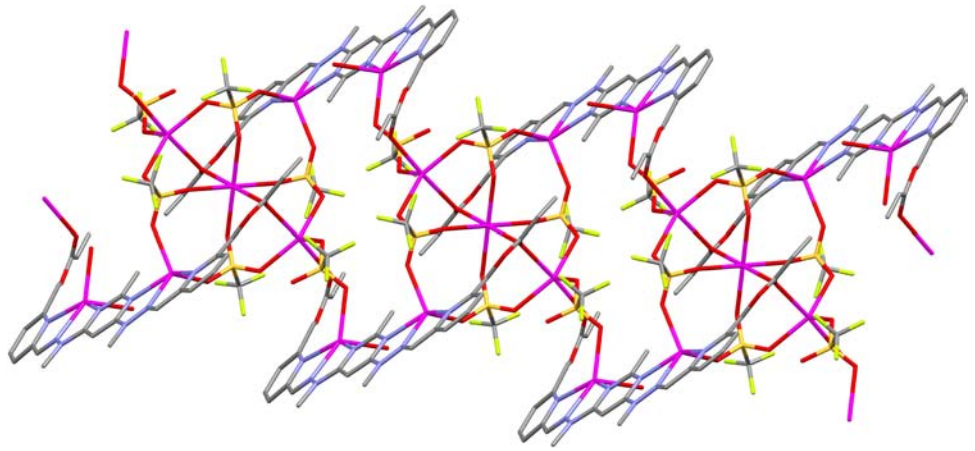

Figure 10. View of the one-dimensional chain arrangement of complex **8** (hydrogens have been omitted for clarity).

Ag(I) ions, of which 2 occupied the coordination pockets of the **L2** ligand, 3.5 $SO_3CF_3^-$ anions, and a H_2O molecule. Due to the noncoordinating nature of the CD_3NO_2 solvent the coordination environments of the Ag(I) ions were satisfied by the **L2** ligand and the $SO_3CF_3^-$ anions.[38] This resulted in a complicated network of coordination bonds which linked all of the contents of the asymmetric unit together, with the exception of the 0.5 $SO_3CF_3^-$ anion (which was removed from the solution by the SQUEEZE command of PLATON[30] due to severe disorder). The *P*-1 symmetry operation gave complex **8** a centrosymmetric dimeric $[Ag_7(\mathbf{L2})_2(SO_3CF_3)_6(H_2O)_2]^+$ structure (Figure 9). These dimers were linked together as a coordination polymer through bonding between the Ag2 ion and the O11-containing $SO_3CF_3^-$ anion and the Ag3 ion and the O4 carbonyl donor of a terminal acryloyl arm (Figure 10).

The **L2** molecules of the $[Ag_7(\mathbf{L2})_2(SO_3CF_3)_6(H_2O)_2]^+$ cation had a linear shape similar to complexes **1**−**7**, with both pym−hyz−py linkages in cisoid−cisoid conformation and a Ag(I) ion occupying each coordination pocket. The centroid to centroid distance between the py rings was 13.81 Å, and the distance between the Ag1 and the Ag2 ions was 6.60 Å. Ag1 and Ag2 both had similarly distorted square pyramidal geometries (τ_5 values of 0.07 and 0.14, respectively),[37] with bonds to the three N donors of the pym−hyz−py pockets. Ag1 was additionally bound to three $SO_3CF_3^-$ anions, while the coordination sphere of Ag2 was completed by a H_2O molecule and a symmetry-generated $SO_3CF_3^-$ anion. Ag3 existed in a distorted five-coordinate trigonal bipyramidal all O donor environment ($\tau_5 = 0.52$)[37] with coordination bonds to three $SO_3CF_3^-$ anions, the O1 carbonyl donor of one of the acryloyl arms of **L2**, and the O4 carbonyl donor on a symmetry-generated $[Ag_7(\mathbf{L2})_2(SO_3CF_3)_6(H_2O)_2]^+$ cation. Ag4 resided on the center of inversion of the *P*-1 space group in a relatively rare elongated octahedral all O donor environment,[34,39] with bonds to the O1 carbonyl donors on each of the **L2** molecules of the $[Ag_7(\mathbf{L2})_2(SO_3CF_3)_6(H_2O)_2]^+$ cation as well as two pairs of symmetry-related $SO_3CF_3^-$ anions (Figure 9).

Ag4 was surrounded by the S2- and S3-containing $SO_3CF_3^-$ anions and their symmetrical equivalents. The three O donors of each of these $SO_3CF_3^-$ anions were bound to Ag1, Ag3, and Ag4 in a monodentate fashion. The S1-containing $SO_3CF_3^-$

dx.doi.org/10.1021/ic3027978 | *Inorg. Chem.* 2013, 52, 2716−2728

bridged the $[Ag_7(\mathbf{L2})_2(SO_3CF_3)_6(H_2O)_2]^+$cations together to form a double-chained polymeric strand as O12 was bound to Ag3 on one cation and O11 was bound to Ag2 on the adjacent cation.

CONCLUSION

The ditopic pym−hyz ligand **L2** was synthesized with terminal acryloyl arms so that it could be incorporated into a copolymer gel through radical polymerization. NMR spectroscopy showed that the ligand had a horseshoe shape with transoid pym−hyz bonds, as expected for a ditopic pym−hyz strand. Reacting **L2** with an excess amount of Pb(II), Zn(II), Cu(II), or Ag(I) ions resulted in isomerization of the pym−hyz bonds from transoid to cisoid conformations and formation of linear complexes. From the NMR spectra of the complexes it appeared that the acryloyl arms were not coordinated to any of the metal ions in solution; however, the crystal structures of complexes **1**, **2**, and **3** showed that in the solid state the carbonyl or alkoxy oxygen donors of the acryloyl arms could coordinate to or at least weakly associate with the metal ions occupying the pym−hyz−py coordination pockets. However, this coordination did not affect the overall linear structure of the complexes of **L2**. Participation of the acryloyl arms did however result in the polymeric structure of complex **8**.

The steric bulk of the acryloyl arms did however influence the outcome of self-assembly at low metal to ligand ratios, resulting in lack of formation of any [2 × 2] grid complexes or double helicates. Instead, reactions of **L2** with Pb(II) and Ag(I) ions in a 1:1 metal to ligand ratio only formed the linear complexes, while a 1:1 metal to ligand ratio with Cu(II) ions resulted in mono-Cu(II) complexes similar to the bent complexes formed with the hydroxymethyl-terminated pym−hyz ligand **L1**. $Zn(\mathbf{L2})_2A_2$ corner complexes were formed when **L2** was reacted with Zn(II) ions in a 4:5 metal to ligand ratio.

It therefore appeared that the influence the terminal acryloyl arms had on the self-assembly of the **L2** complexes was purely steric in nature. The fact that their presence did not inhibit coordination of metal ions to the pym−hyz−py pockets or subsequent transoid to cisoid isomerization of the pym−hyz bonds suggested that ligands such as **L2** would be appropriate for inclusion in a polymer gel actuator.

ASSOCIATED CONTENT

Supporting Information

Discussion of how the disorder of complexes **1**−**8** was treated, pictorial views of complexes **1**−**8** showing thermal ellipsoids at the 50% probability level, as well as selected bond lengths and angles for complexes **1**−**8** in tabulated form; X-ray crystallographic data in CIF format. This material is available free of charge via the Internet at http://pubs.acs.org.

AUTHOR INFORMATION

Corresponding Author

*E-mail: lhanton@chemistry.otago.ac.nz.

Notes

The authors declare no competing financial interest.

ACKNOWLEDGMENTS

We thank the Department of Chemistry, University of Otago, and the New Economic Research Fund of the Foundation for Research, Science and Technology (NERF Grant No. UOO-X0808) for financial support.

REFERENCES

(1) Stadler, A.-M.; Kyritsakas, N.; Graff, R.; Lehn, J.-M. *Chem.—Eur. J.* **2006**, *12* (17), 4503−4522.
(2) (a) Schmitt, J.-L.; Stadler, A.-M.; Kyritsakas, N.; Lehn, J.-M. *Helv. Chim. Acta* **2003**, *86* (5), 1598−1624. (b) Gardinier, K. M.; Khoury, R. G.; Lehn, J.-M. *Chem.—Eur. J.* **2000**, *6* (22), 4124−4131.
(3) Ramírez, J.; Stadler, A.-M.; Harrowfield, J. M.; Brelot, L.; Huuskonen, J.; Rissanen, K.; Allouche, L.; Lehn, J.-M. *Z. Anorg. Allg. Chem.* **2007**, *633* (13−14), 2435−2444.
(4) Giuseppone, N.; Schmitt, J.-L.; Lehn, J.-M. *J. Am. Chem. Soc.* **2006**, *128* (51), 16748−16763.
(5) (a) Chaur, M. N.; Collado, D.; Lehn, J.-M. *Chem.—Eur. J.* **2011**, *17* (1), 248−258. (b) Stefankiewicz, A. R.; Rogez, G.; Harrowfield, J.; Drillon, M.; Lehn, J.-M. *Dalton Trans.* **2009**, *29*, 5787−5802. (c) Barboiu, M.; Ruben, M.; Blasen, G.; Kyritsakas, N.; Chacko, E.; Dutta, M.; Radekovich, O.; Lenton, K.; Brook, D. J. R.; Lehn, J.-M. *Eur. J. Inorg. Chem.* **2006**, *6*, 784−792. (d) Tielmann, P.; Marchal, A.; Lehn, J.-M. *Tetrahedron Lett.* **2005**, *46* (37), 6349−6353.
(6) Uppadine, L. H.; Lehn, J.-M. *Angew. Chem., Int. Ed. Engl.* **2004**, *43*, 240−243.
(7) Stefankiewicz, A. R.; Harrowfield, J.; Madalan, A.; Rissanen, K.; Sobolev, A. N.; Lehn, J.-M. *Dalton Trans.* **2011**, *40* (45), 12320−12332.
(8) Parizel, N.; Ramírez, J.; Burg, C.; Choua, S.; Bernard, M.; Gambarelli, S.; Maurel, V.; Brelot, L.; Lehn, J.-M.; Turek, P.; Stadler, A.-M. *Chem. Commun.* **2011**, *47* (39), 10951−10953.
(9) Cao, X.-Y.; Harrowfield, J.; Nitschke, J.; Ramirez, J.; Stadler, A.-M.; Kyritsakas-Gruber, N.; Madalan, A.; Rissanen, K.; Russo, L.; Vaughan, G.; Lehn, J.-M. *Eur. J. Inorg. Chem.* **2007**, *18*, 2944−2965.
(10) Stadler, A.-M.; Kyritsakas, N.; Vaughan, G.; Lehn, J.-M. *Chem.—Eur. J.* **2007**, *13* (1), 59−68.
(11) Yoshida, R. *Adv. Mater.* **2010**, *22* (31), 3463−3483.
(12) (a) Mirfakhrai, T.; Madden, J. D. W.; Baughman, R. H. *Mater. Today* **2007**, *10* (6), 30−38. (b) Baughman, R. H. *Science* **2005**, *308* (5718), 63−65. (b) Hu, Z.; Zhang, X.; Li, Y. *Science* **1995**, *269* (5223), 525−527. (c) Osada, Y.; Okuzaki, H.; Hori, H. *Nature* **1992**, *355* (6357), 242−244.
(13) Bassetti, M. J.; Chatterjee, A. N.; Aluru, N. R.; Beebe, D. J. *J. Microelectromech. Syst.* **2005**, *14* (5), 1198−1207.
(14) (a) Wei, J.; Yu, Y. *Soft Matter* **2012**, *8* (31), 8050−8059. (b) Schneider, H.-J.; Strongin, R. M. *Acc. Chem. Res.* **2009**, *42* (10), 1489−1500. (c) Tanaka, T. *Phys. Rev. Lett.* **1978**, *40* (12), 820−823.
(15) (a) Swift, G. *Acrylic (and methacrylic) Acid Polymers. From Encyclopedia of Polymer Science and Technology*; John Wiley & Sons Inc.: Hoboken, 2004. (b) Coote, M. L.; Davis, T. P. *Copolymerization Kinetics. From Handbook of Radical Polymerization*; John Wiley & Sons Inc.: Hoboken, 2002.
(16) Hutchinson, D. J.; Cameron, S. A.; Hanton, L. R.; Moratti, S. C. *Inorg. Chem.* **2012**, *51* (9), 5070−5081.
(17) Hutchinson, D. J.; Hanton, L. R.; Moratti, S. C. *Inorg. Chem.* **2011**, *50* (16), 7637−7649.
(18) Hutchinson, D. J.; Hanton, L. R.; Moratti, S. C. *Inorg. Chem.* **2010**, *49* (13), 5923−5934.
(19) (a) Dawe, L. N.; Shuvaev, K. V.; Thompson, L. K. *Chem. Soc. Rev.* **2009**, *38* (8), 2334−2359. (b) Dawe, L. N.; Thompson, L. K. *Dalton Trans.* **2008**, *27*, 3610−3618.
(20) (a) Price, J. R.; White, N. G.; Perez-Velasco, A.; Jameson, G. B.; Hunter, C. A.; Brooker, S. *Inorg. Chem.* **2008**, *47* (22), 10729−10738. (b) Caradoc-Davies, P. L.; Hanton, L. R.; Lee, K. *Chem. Commun.* **2000**, *9*, 783−794.
(21) (a) Allen, F. H. *Acta. Crystallogr., Sect. B: Struct. Sci.* **2002**, *B58*, 380−388. (b) Allen, F. H.; Davies, J. E.; Galloy, J. J.; Johnson, O.; Kennard, O.; Macrae, C. F.; Mitchell, E. M.; Mitchell, G. F.; Smith, J. M.; Watson, D. G. *J. Chem. Inf. Model.* **1991**, *31* (2), 187−204.
(22) Hutchinson, D. J.; Hanton, L. R.; Moratti, S. C. *Acta. Crystallogr., Sect. E: Struct. Rep. Online* **2009**, *E65* (7), o1546.
(23) Kuwabara, J.; Takeuchi, D.; Osakada, K. *Chem. Commun.* **2006**, *36*, 3815−3817.

(24) (a) Otwinowski, Z.; Minor, W. Processing of X-Ray Diffraction Data Collected in Oscillation Model. In *Methods in Enzymology*; Carter, C. W., Jr., Sweet, R. M., Eds.; Academic Press: New York, 1997; Vol. *276*, pp 307−326. (b) *SAINT V4, Area Detector Control and Integration Software*; Siemens Analytical X-Ray Systems Inc.: Madison, WI, 1996.
(25) Sheldrick, G. M. *SADABS, Program for Absorption Correction*; University of Göttingen: Göttingen, Germany, 1996.
(26) Sheldrick, G. M. *Acta Crystallogr., Sect. A* **1990**, *46*, 467−473.
(27) Altomare, A.; Burla, M. C.; Camalli, M.; Cascarano, G. L.; Giacovazzo, C.; Guagliardi, A.; Moliterni, A. G. G.; Polidori, G.; Spagna, R. *J. Appl. Crystallogr.* **1999**, *32*, 115−119.
(28) Sheldrick, G. M. *SHELXL-97, Program for the Solution of Crystal Structures*; University of Göttingen: Göttingen, Germany, 1997.
(29) Farrugia, L. J. *J. Appl. Crystallogr.* **1999**, *32*, 837−838.
(30) Spek, A. L. *Acta Crystallogr., Sect. A* **1990**, *46*, C34.
(31) (a) Macrae, C. F.; Edgington, P. R.; McCabe, P.; Pidcock, E.; Shields, G. P.; Taylor, R.; Towler, M.; van de Streek, J. *J. Appl. Crystallogr.* **2006**, *39*, 453−457. (b) Bruno, I. J.; Cole, J. C.; Edgington, P. R.; Kessler, M. K.; Macrae, C. F.; McCabe, P.; Pearson, J.; Taylor, R. *Acta Crystallogr., Sect. B* **2002**, *58*, 389−397.
(32) Alkorta, I.; Elguero, J.; Roussel, C. *Comput. Theor. Chem.* **2011**, *966* (1−3), 334−339.
(33) (a) Hathaway, B. J. *Dalton. Trans.* **1972**, *12*, 1196−1199. (b) Hathaway, B. J. *Copper. From Comprehensive Coordination Chemistry: The synthesis, reactions, properties & applications of coordination compounds*; Pergamon Books Ltd.: Oxford, 1987; Vol. *5*.
(34) Argyle, V. J.; Woods, L. M.; Roxburgh, M.; Hanton, L. R. *CrystEngComm* **2013**, *15*, 120−134.
(35) (a) Masoomi, M. Y.; Morsali, A. *Coord. Chem. Rev.* **2012**, *256* (23−24), 2921−2943. (b) Leong, W. L.; Vital, J. J. *Chem. Rev.* **2011**, *111* (2), 688−764. (c) Cordes, D. B.; Hanton, L. R.; Spicer, M. D. *Inorg. Chem.* **2006**, *45* (19), 7651−7664.
(36) (a) Harrowfield, J. *Helv. Chim. Acta* **2005**, *88* (9), 2430−2432. (b) Shimoni-Livny, L.; Glusker, J. P.; Bock, C. W. *Inorg. Chem.* **1998**, *37* (8), 1853−1867.
(37) Addison, A. W; Rao, T. N.; Reedijk, J.; van Rijn, J.; Verschoor, G. C. *Dalton Trans.* **1984**, *7*, 1349−1356.
(38) (a) Gimeno, N.; Vilar, R. *Coord. Chem. Rev.* **2006**, *250* (23−24), 3161−3189. (b) Bu, X.-H.; Chen, W.; Hou, W.-F.; Du, M.; Zhang, R.-H.; Brisse, F. *Inorg Chem.* **2002**, *41* (13), 3477−3482.
(39) Young, A. G.; Hanton, L. R. *Coord. Chem. Rev.* **2008**, *252* (12−14), 1346−1386.